

Enhancement of The Solar Energy Harvesting System for WSN Nodes Through INC-MPPT

Praveen Singh Rajput

M.Tech Scholar, Department of Computer Science & Engineering, Vishveshwarya Group of Institutions, Gautam Buddh Nagar, India.

Mrs. Madhu Lata Nirmal

Assistant Professor, Department of Computer Science & Engineering, Vishveshwarya Group of Institutions, Gautam Buddh Nagar, India.

Abstract

These days, one of the most exciting areas of research is focused on solar photovoltaic power generation systems. Even national governments are making plans to increase the proportion of power generation that comes from renewable energy sources. This is due to the fact that the viability and crisis of conventional energy sources are expected to increase in the future. Solar energy is a sustainable and environmentally friendly kind of energy production. In recent years, research in the Internet of Things has focused on putting WSNs to use in conjunction with solar energy collecting techniques. The battery energy of a WSN node is very low, and its lifespan can be measured in just a few days at most depending on the working duty cycle. In this research, we propose a new SEH approach that can be used for WSN nodes that have limited energy resources. Nodes that are part of a Solar Energy Harvesting Wireless Sensor Network (SEH-WSN) will typically continue to function for many years to come. P&O Maximum Power Point Tracking (MPPT) was the method that was utilised in the development of solar energy harvesting in the past, and it was quite successful. This led to the harvesting of solar energy. INC (Incremental Conductance), on the other hand, does yield effects that are superior to P&O. In order to implement the SEH-WSN method, we are making use of the INC-MPPT technique, and we are contrasting it with the P&O-MPPT methodology.

Index Terms—Solar energy harvesting, INC, MPPT, DC-DC Converter.

I. INTRODUCTION

The remote sensor network is a fundamental component of the Internet of Things (IoTs) (WSN). These organizations have been extensively deployed in a variety of applications, including security in the military, disaster recovery, patient health monitoring, air quality monitoring, and so on [1]. The demand for devices that can operate on their own power has been sparked by recent developments in late-stage remote technology. This is evident, in particular with regard to the organization of remote sensors (WSN). This can be improved by

harvesting energy from the environment as a whole, for as by orienting solar panels toward the sun or wind turbines, etc. These energy harvesting devices have the capability to control remote sensor hubs either directly or via connecting to a battery [2]. The WSN hubs are hampered by the effects of a major plan essential in the sense that their battery power is restricted, and they are only able to function for a number of days at most, depending on the activity pattern of the obligation [3].

The energy that is generated from sunlight is often stored in solar cells; therefore, the capacity for energy storage needs to be increased. Through the photovoltaic effect, solar power can be rapidly converted into usable electricity by deploying photovoltaic (PV) boards [4]. Regardless of this, the productivity of the transformation is low, and the cost of the developed intensity is comparable to that of a high cost. PV technology offers a number of advantages, some of which are that it has low fuel costs, does not contribute to the creation of pollution, calls for relatively little maintenance, and PV frameworks have a greater variety of features [5]. The term "sunlight-based photovoltaic" (PV) energy collection refers to the conversion of light energy from the sun into electrical energy, which can then be used to power an electronic or electrical device.

When it comes to wireless sensor networks (WSNs), light energy from the sun is converted into electrical energy and then used to recharge the battery of a WSN hub at the location where the activity is taking place [6]. In this method, once the energy stored in the battery has been drawn out, it will be necessary to continually replace the batteries. It is possible to control a WSN hub with the electrical energy that is generated from solar power, and this is a perfectly lawful use of this energy. On the other hand, the amassed power may be stored in a battery-operated battery for use at a later time.

The Self-Contained Energy Harvesting Wireless Sensor Networks (SEH-WSNs) are made up of miniature self-sufficient WSN hubs that are connected to little sunlight-based boards for their energy gathering needs. It has been determined that the maximum amount of power that could be gathered from solar-powered energy while in the open air is 15 mW/cm², with productivity reaching up to 30 percent [7]. As a result, we have decided to gather energy from the sun in order to provide supplementary capacity to the WSNs because this method offers the greatest potential for powerful thickness and large productivity.

There have been many different strategies offered [8] to follow the purpose of a PV module that requires the most extreme force possible in order to beat the restriction of efficacy. The maximum power point tracking (MPPT) technique is applied to solar photovoltaic (PV) modules so that the maximum amount of energy can be extracted from them and then stored.

The DC-DC converter acts as an interface between the heap and the PV module, effectively transferring the most power from the solar-powered PV module to the heap. It does this by converting direct current to direct current. Changing the obligation cycle allows the load impedance to be matched up with the source impedance, which allows for the most possible force to be extracted from the PV panel [9]. In this section, the INC-MPPT and P&O-MPPT approaches are compared with regard to their efficiencies, and the best possible outcome will be shown.

II. LITERATURE REVIEW

The energy generated by photovoltaic panels is taken in by power system networks using methods for matrix related inverters. In PV power systems, one of the most significant issues is that there is often no coordination between the operational particulars of the PV clusters and the storage areas, which is a common occurrence. In particular, the PV Module exhibit demonstrates a non-direct style for the V-I bend and the greatest force point on the V-P bend when subjected to a variety of ecological states. The productivity of PV modules falls somewhere in the range of 10 to 25 percent.

This indicates that calculations for greatest force point following (MPPT) are incorporated into the overall framework in order to increase the capacity of the modules and lower their overall cost.

The technological advancement in wireless communication has led to the development of wireless sensor networks. With the exceptional capability of not only sensing but processing as well, wireless sensor networks became popular and very much required for many applications. Sensor nodes are small and they are deployed in the monitoring area in large amount to detect events. But Sensor nodes are resource constrained. They are tiny nodes with limited storage capacity, low cost processor, and limited transceiver range and with limited battery lifetime. Sensor nodes sense the monitoring area such as forests, a field, underwater, cities, human body etc. and transmit the sensed data to the sink.

This transmission may take place via single-hop or through multi-hops. In single-hop networks nodes can directly send data to the sink. But generally, a sensor network field is large and the nodes transmission range is limited, so the nodes may send data to the sink via intermediate nodes or forwarding nodes, which is called as the multi-hop network [38].

Sensor nodes deplete their energy due to direct data transmission in single hop whereas in a multi-hop, the forwarding nodes deplete their energy and reduce the network lifetime. The lifetime of sensor nodes mainly depends upon a finite source of energy like battery. Therefore, it is crucial to consider the energy efficient techniques to increase the life span of the network. Heinzelman et al., (2000) discussed Low Energy Adaptive Clustering Hierarchy (LEACH) protocol in which nodes in the network are divided into clusters. Nodes that are more proximate to the Cluster Head join the respective cluster only when they receive strong signal strength. Data transmits from nodes to the base station via cluster head, which are randomly chosen. Cluster Head aggregates and compresses the data using different techniques and then forwards the data to the sink. Since CHs are randomly chosen, any node can get a chance to become a Cluster Head in the entire network.

LEACH uses distributive clustering mechanism which consequently leads to efficient energy utilization and longer lifetime of the network. It consists of two phases- steady state and setup phase. In steady state phase, sensor nodes join the cluster based on the signal strength received from the nearest CH. The TDMA slot has also been assigned to the sensor nodes in the cluster. In the steady state phase, the sensor nodes send their sensed data to the CH in their respective slot and then CH sends the processed data to the Base station. LEACH is not felicitous for large networks since nodes directly transmit data to the Base station and Cluster Head. Enhancement in LEACH includes TL-LEACH [32], E-LEACH [33], M-LEACH, LEACH-C [31], etc.

Actual load balancing cannot be presented in LEACH. Also, dynamic clustering brings extra overhead.

Bandyopadhyay et al., (2003) discussed a clustering protocol, with each cluster having a head node called cluster head. Sensors communicate information to cluster heads only which then communicate to the base station. Such a design may help increase WSN lifetime by saving energy. They compare several clustering algorithms and propose a fast, distributed and randomized clustering algorithm to organize the sensors in a WSN. This algorithm is shown to have lesser complexity and more energy savings.

The authors have used stochastic geometry to arrive at values of parameters for the algorithm that minimize the energy spent in the WSN, specifically by minimizing the communications to the base station. The authors also report that energy savings increases with the number of levels in the hierarchy of clusters. The proposed algorithm is said to be suitable for networks of a large number of nodes.

Qing et al., (2006) have introduced Distributed Energy Efficient Clustering (DEEC) algorithm for heterogeneous WSNs. In heterogeneous network, all nodes have different levels of energy and the distributed nature of the network protects single point failure. In DEEC, like LEACH, the CH role is rotated among all the nodes in the network. CHs are chosen based on residual energy and average energy of the network. Nodes with high initial energy and residual energy have a high probability to become a CH. DEEC assigns different epoch for each round of selection of cluster head by considering both the initial and residual energy. Residual energy is calculated on the basis of ideal value of a network lifetime and global knowledge of the network is not required by each node. DEEC controls the equal dissipation of energy in each round by controlling the rotating epoch in accordance with the current energy level and average energy of the network as the reference energy. Hence, nodes die at the same time.

DEEC results are more significant in terms of energy efficiency and longer lifetime of network than the other algorithms it is compared with. But advanced nodes always punished to become CH. Although after some rounds, the energy of advanced nodes is equal to that of normal nodes. Other limitation of DEEC is that the average energy is not directly proportional to the energy consumed in all iterations.

Lotf et al., (2008) introduced Extended Lifetime of Cluster Head (ELCH) that confirmed better results in terms of energy efficiency as compared with LEACH. It is a distributed protocol that combines multi-hop routing and cluster architecture for achieving the energy efficiency. Cluster heads collect the data and send it to the BS via intermediate nodes. Nodes in the clusters are chosen based on their location i.e. nodes which receive stronger signal strength are selected. Each node forwards the data directly to the cluster head.

Yong, Z. et al., (2012), The Authors claim that their proposed clustering algorithm DECSA (Distance-Energy Cluster Structure Algorithm) is an alternative to LEACH that prolongs 31% of network lifetime, reduces 40% of the energy consumption and has a better overall performance than the original LEACH protocol. Their critique of LEACH is that it does not consider the location and residual energy of nodes which leads to overall inefficiency in the network. DECSA, on the other hand, considers both distance and residual energy of the nodes. The node with greater residual energy is elected as the cluster head and their algorithm optimizes high power communication between cluster head and the base station. Cluster head is selected in two phases- 1) Election of an ordinary cluster head node 2) Election of base

station cluster head node (CH closest to the Base station is BCH). In first phase, false cluster head nodes are selected based on a threshold value by considering distance and residual energy. If the random value is smaller than the threshold value, then it is considered as a CH node. In the next round of CH, if the threshold value of all nodes in the cluster is greater than the false CH value, then it is designated as CH.

In second phase, BCH are selected on the basis of a threshold value and if value is greater than the predefined threshold, Base station broadcasts the message and the CH, which has the maximum value of threshold, will be considered as next hop by the BCH. This way, it connects to the CH and forms a complete path to the destination and reduces the energy consumption of CH nodes with low residual energy.

Nikolidakis et al., (2013), This research paper acknowledged that WSNs are used in a very wide variety of applications such as agriculture, traffic control, environment and habitat monitoring, object tracking, fire detection, surveillance and reconnaissance, home automation, biomedical applications, inventory control, machine failure diagnosis and energy management. However, the use of WSNs is severely limited due to lack of energy management. This work proposes a routing algorithm termed ECHERP (Equalized Cluster Head Election Routing Protocol), which pursues energy conservation through balanced clustering in a homogeneous environment. These are compared in a detailed manner with existing algorithms of LEACH, PEGASIS, and BCDCP. ECHERP models the network as a linear system and computes the combination of nodes that can be chosen as cluster heads in order to extend the network lifetime. Cluster head selection is done through Gaussian elimination method in two steps.

The BS calculates the number of rounds for which a node can become a CH. Re-clustering process is not carried out which minimizes the energy wasted. For maximizing the network lifetime, current energy levels and estimated future residual energy levels of nodes are considered. Upper level CH nodes and lower level CH nodes are selected which establish the energy efficiency of their algorithm through simulation tests. But, multi-hop CH selection by BS and application of Gaussian elimination algorithm makes the design complex.

Lee et al., (2016) discuss the improvement in Leach protocol. LEACH (Low Energy Adaptive Clustering Hierarchy) is an algorithm that divides the entire network into a random cluster and manages by forming the head for each cluster. The Dual Hop method is used during transmission of LEACH to reduce the energy consumption of cluster heads for remote transmission and to increase the energy efficiency of sensor nodes. DL-LEACH changes the previous transmission method of LEACH to a dual hop (single-hop + multi-hop) transmission method. The multi-hop transmission of DL-LEACH is made of layer units. The member nodes send the data to the closest CH. The cluster head of DL-LEACH transmits its data to the closest cluster head near the lower level. This layer consolidates the above information with its own information and sends it to the lower layer. If a cluster head is absented in this layer then the data is sent to the Base Station. This way, the process uses both single-hop and multi-hop.

Smaragdakis et al. [41] are known for a Stable Election Protocol (SEP) which is a variation of LEACH. It is designed mainly for dual level heterogeneous networks composed of doublet types of sensors (particularly Advance and normal nodes). In general, advance sensors retain extra energy and this has to be turned CH's more frequently compared to normal nodes. Here CH's chosen pertain to sensors initial energy. The main disadvantage is that this decision of CH's is not dynamic. As a consequence, advanced nodes that are far flung with reference to the

sink drain their energy faster and depart from their existence soon. SEP is not suitable for multilevel heterogeneous network.

Malluh et al. [42] have suggested an improved form of SEP. Here also, advanced nodes are selected as CH's more often than the normal sensors. In addition, the number of nodes connected with each CH is considered. Thus enables equitable distribution for the sensor nodes between the CH's. Also, in the event of an excess of one sensor accessible to be a CH at certain round, EM-SEP chooses the higher energy sensor as a CH. Those two factors protract the stable period of the sensor network. The main drawback in this method is that inter-cluster communication cost is not considered.

Georgious et al. [42], propose Stable Election Protocol (SEP), a heterogeneous-aware protocol to prolong the stability period and average throughput. SEP is based on weighted election probabilities of nodes to become CH according to the residual energy. Nodes are divided into two categories; based on their energy one are advanced nodes and other are normal nodes advanced node have more energy than normal nodes. The probability to become cluster head of advanced node is more than normal nodes.

III. PV MODEL WITH PARAMETERS

When it comes to the construction of solar cells, the semiconductor material that is used most frequently is silicon. Valence electrons are present in the silicon molecule in four different positions. Every single silicon atom in a hard precious stone shares each of its four valence electrons with another silicon particle that is physically nearest to it. This results in the formation of covalent links between the silicon atoms. In this manner, the cross-sectional structure of the silicon precious stone is given the form of a tetrahedron. When a light beam impacts any substance, a portion of the light is reflected, a portion of the light is transmitted through the medium, and the remaining light is absorbed by the material. When light is shone on a silicon precious stone, a phenomenon quite similar to this one takes place. In the event that the power of the incident light is sufficiently great, adequate quantities of photons are consumed by the gem, and these photons, in turn, activate a portion of the electrons that are associated with the covalent bonds. At that point, the electrons that were previously excited obtain sufficient energy to transition from the valence band to the conduction band. Because the energy level of these electrons is in the conduction band, they depart the covalent bond, leaving behind a hole in the bond for each electron that they eliminate. These electrons, which are referred to as "free electrons," wander around at will within the precious stone structure of the silicon. These apertures and free electrons are extremely important components in the process of producing power in a solar cell. These electrons and apertures are referred to as light-created electrons and openings respectively from this point forward. These light-created electrons and apertures are not capable of delivering power by them within the silicon gem. It seems like there ought to be an additional way for doing that.

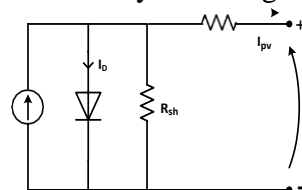


Figure 1: Single diode model of PV cell

Figure 1 is a PV cell in which one current source, one forward bias diode, 2 resistances are connected.

The electron-hole pair (EHP) is produced Incident of a photon of light energy ($h\nu > E_g$) over a solar cell. The newly created EHP relates to electric current denoted by (IL) termed light induced current. The ideal equation of a solar cell with current-voltage (I – V) is given as

$$\text{Solar Cell Current } (I) = I_{ph} - I_0 \left[\exp\left(\frac{qV}{kT}\right) - 1 \right] \quad (1)$$

Where, I = solar cell output current, I_{ph} = light produced by solar cell, I_0 = Reverse current of saturation because of recombination, q = electron charge (1.6×10^{-19} C), V = Open-circuit voltage of solar cell, k= Boltzmann constant (1.38×10^{-23} J/ K), T = solar cell temperature (300 K).

The circuit model in figure 1 represents equivalent of solar cell. It comprises light-produced source current (I_{ph}), a Shockley equation-modeled diode (D), and two series and parallel resistances. Figure 3.11 shows the VI and PV characteristic in which on voltage shows and on y axis current left side and power right side shows.

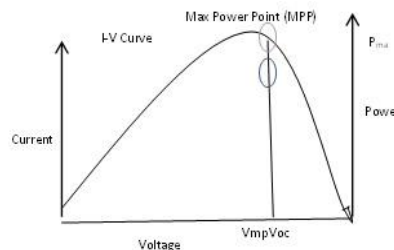


Figure 2: V-I and P-V Characteristic

The maximum power point (MPP) is a point on the Power voltage (P-V) characteristic of the solar cell, where the maximum power can be extracted from the solar cell as shown in Figure 2. Ideally, the solar cell efficiency should be high. But practically, it is limited to 5%–15% only (Green, M. A., Hishikawa, 2018).

In Figure 2, the current law of Kirchoff (KCL) can provide characteristic equation of current for that corresponding circuit:

$$\text{Equivalent Cell Output Current } (I) = I_{ph} - I_D - I_P \quad (2)$$

Where, I_P = parallel resistance current, I_{ph} = Light produced current, and I_D = diode current.

$$\text{Diode Current } (I_D) = I_0 \left[\exp\left(\frac{V+I_p R_s}{nV_T}\right) - 1 \right] \quad (3)$$

Where, I_0 = Reverse Saturation current because of recombination, V = solar cell open circuit voltage, R_s = series resistance, I_p = solar cell output current, n = diode norm factor, (1 termed as ideal, 2 termed as practical diode), k = Boltzmann constant (1.38×10^{-23} J/K), V_T = Thermal voltage (kT/q), T = Solar cell Temperature (300 K). Q = electron charge (1.6×10^{-19} C). The parallel-resistance current is determined as:

$$\text{Current in parallel resistance } (I_p) = \frac{V+I_p R_s}{R_p} \quad (4)$$

Now, by placing the I_D and I_p value in the equation (4), we obtain complete equivalent circuit fourth equation of solar cell, under that all values are defined as connected with output current and voltage [9]:

$$Solar\ Cell\ Current\ (I) = I_L - I_0 \left[\exp \left(\frac{q(V + I_p v R_s)}{nkT} \right) \right] - \left(\frac{V + I R_s}{R_p} \right) \quad (5)$$

Where, R_p = Parallel Resistance and in Equation (5), the other parameters I_0 , I_L , V , I , q , R_s , n , k , T were already declared. The solar cell efficiency (η) is termed as:

$$Solar\ Cell\ Efficiency\ (\eta) = \frac{V_{oc} I_{sc} FF}{P_{in}} \quad (6)$$

Where I_{sc} is Current Short Circuit, V_{oc} is called Open Circuit Voltage, FF = Fill Factor and P_{in} = optical incident power. A Solar Cell's Fill Factor (FF) is given as

$$Fill\ Factor\ (FF) = \frac{P_{max}}{P_{dc}} = \frac{I_m V_m}{I_{sc} V_{oc}} \quad (7)$$

Where V_m is the solar cell's maximum voltage and I_m is called maximum current. There are practically many kinds of solar cells, like amorphous silicon solar cells (a-Si), mono-crystalline silicon solar cells (C-Si), thin film solar cells (TFSC), polycrystalline solar cells (multi-Si) etc. But the productivity of a-Si solar cells is greater than any other efficiency till 18 per cent.

➤ **Solar Radiation Effect (G)**

The efficiency of solar cell (η) is proportional to solar radiations variations. The efficiency of solar cell (η) increases, on increasing the solar radiation and vice versa. Figure 3 (a) displays the current-voltage (I–iV) properties of a commercial solar panel of 10 watts with varying values of irradiance.

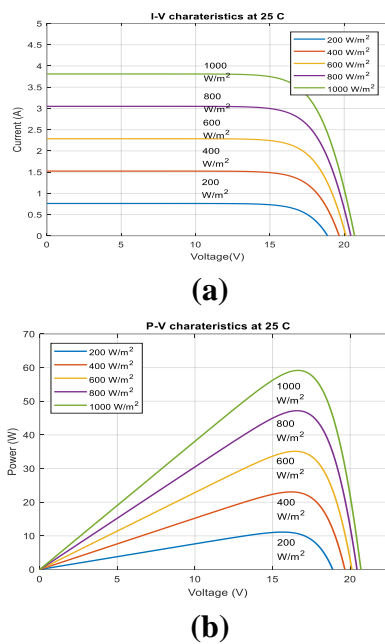


Figure 3: Solar Panel characterization with Irradiance level variations ($Watts/m^2$). (a) Characteristics of (I–V) (b) Characteristics of (P–V)

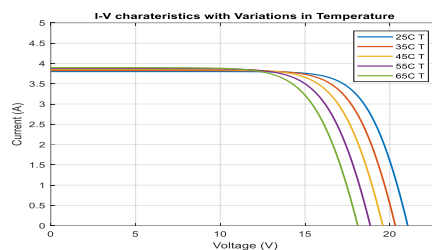
The solar panel with a capacity of 10 watts (Dow Chemical DPS 10–1000) measures 232 millimetres * 546 millimetres and has a module area of 0.13 square metres. It can be seen from looking at Figure 3 (a) that the amount of irradiance produces a correlation that leads to an increase in the solar panel current. Here, the solar cell current is at its optimal level for the sun irradiation of 1000 W/m^2 (6.2 A). Figure 3b illustrates how the power-voltage characteristics

of a solar panel change depending on the amount of radiation. The amount of power that is extracted is at its peak when there is a sun irradiation of 1000. (9.8 W).

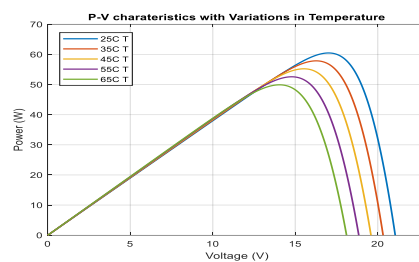
The irradiance variation IV characteristic of a solar panel is depicted in Figure 3 (a), where the x-axis represents voltage and the y-axis represents current. Figure 3b's x-axis represents voltage, while the y-axis represents power.

➤ **The Temperature Effect (T)**

The production value of a solar panel, such as the one shown in Figure 4 (a), will drop if the temperature of the panel rises, and the opposite will be true if the temperature falls. The rise in output, meanwhile, is directly proportional to the varying degrees of temperature. In a similar fashion, the drop in output capacity seen in Figure 4 (b) can be attributed to a rise in temperature, and vice versa. As a result, there is an inverse relationship between the fluctuations in temperature and the output power.



(a)



(b)

Figure 4: Characteristics of solar panels with Temperature (°C) variations. (a) Characteristics of (I–V); (b) Characteristics of (P–V)

Figure 4 (a) and (b) shows characteristic of solar panel with temperature variation in figure (a) x axis is voltage and y axis is current, in figure (b) x axis is voltage and y axis is power.

➤ **Systems for Harvesting Solar Energy**

A rechargeable battery, solar panel, DC-DC converter, Battery Management System (BMS) safety charging circuit, and DC-DC converter control unit are the components that make up a straightforward solar energy harvesting system. The control methods for DC-DC converters are typically maximal power point tracking control (MPPT). Figure 3.14 shows a SEH unit that is equipped with a rechargeable battery, a DC-DC buck converter, a maximum power point (MPPT) solar panel and transmitter, and a WSN sensor node that is coupled to the DC.

Solar panels are used to gather the sun's rays, which are then converted into usable electricity. The DC-DC Buck converter is switched off, which results in the magnitude of the voltage being controlled and then transmitted to the same rechargeable unit. A Maximum Power Point

Tracking sensor is responsible for regulating the current and voltage output of a solar panel by adjusting the duty cycle of a Buck MOSFET DC-DC converter (Mathews, I., King, 2015).

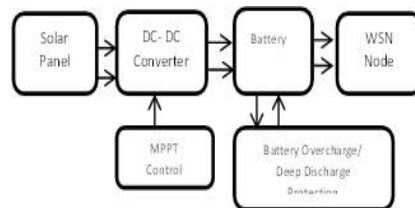


Figure 5: Solar energy recovery (harvesting) system block diagram, using input from MPPT capacity

The block diagram of the solar energy harvest is shown in Figure 5. It consists of a DC-DC converter, battery, WSN node, solar panel, and other components. Last but not least, the voltage of the batteries serves as the governing factor for the wireless sensor node. The WSN is responsible for discovering, analyzing, and interacting with other nodes that share the same characteristics in order to fulfill its duty. Therefore, the SEH-WSN nodes can be used to track and control any physical phenomenon on their own, just like they can be used to monitor and regulate vibration, temperature, acceleration, and humidity. Within the context of this scenario, the effectiveness of the solar harvester circuit demonstrates a very important function. In the event that the performance of the solar power harvester is inadequate, the battery will not be sufficiently recharged; as a result, the wireless sensor network will have a shorter lifespan.

IV. MAXIMUM POWER POINT TRACKING (MPPT) MODELING TECHNIQUE

MPPT techniques (Hauke, B. (2009) are most commonly used in the formation of solar photovoltaic (PV) systems to get the maximum extraction of power from the sun under a variety of solar irradiance values. MPPT techniques are a kind of algorithm that continuously tests the current (IPV) and voltage (VPV) from the solar panel and computes the quantity of the duty cycle (D) for supplying to DC-DC buck converter MOSFET switch. In applications involving photovoltaics, the algorithms listed below are often utilized (Texas, 2018),

- Incremental Conductance (INC)
- Fraction Open Circuit Voltage (OCV).
- Perturb and Observe (P&O)

The P&O method is the primary technique that is applied in all different kinds of solar energy harvester systems. The P&O algorithm's flow diagram can be found in Figure 8. The output of this algorithm has a duty cycle (DD) fluctuation that varies depending on the irradiance (W/m^2) that it receives as input. If there is a drop in irradiance, there will be a shift in the service cycle, as well as changes in the solar panel's voltage and current (Haque, A. 2014). This change is detected by the MPPT technology, which then changes the impedance of the solar panel to achieve maximum power output. Therefore, maximum power (P) may continue to be extracted by the solar panel even if there is a change in the irradiance. It generates a PWM waveform with an initial duty cycle of 0.7 (range from 0 to 1) and uses that value as the seed for the simulation.

The P&O approach is predicated on the principle of achieving balanced impedance between the charge and the solar panel. It is essential to match the impedance in order to have the best power transfer. This impedance matching is achieved by the utilization of a DC-DC converter. Impedance can be altered by using a DC-DC converter, and this is accomplished by modifying the service cycle of the MOSFET switch (DD). The following expressions give the input voltage, output voltage, and duty cycle:

$$V_o = V_{in}.D \tag{8}$$

$$R_{in} = R_L/D^2 \tag{9}$$

In contrast, if the duty cycle is not constant (DD), then the output voltage of the solar energy harvester will shift (Vo). Therefore, an increase in the output voltage, denoted by Vo, takes place whenever the duty cycle, denoted by D, is extended, and vice versa. By modifying the duty cycle (D), which allows for the most effective and efficient transfer of power from the solar panel to the load, it is possible to make a comparison between the impedance of the load resistance (RL) and the impedance of the solar panel input.

The steps in the P&O method are illustrated in a flowchart, and the MATLAB codes corresponding to those phases are shown in Algorithm-1 correspondingly.

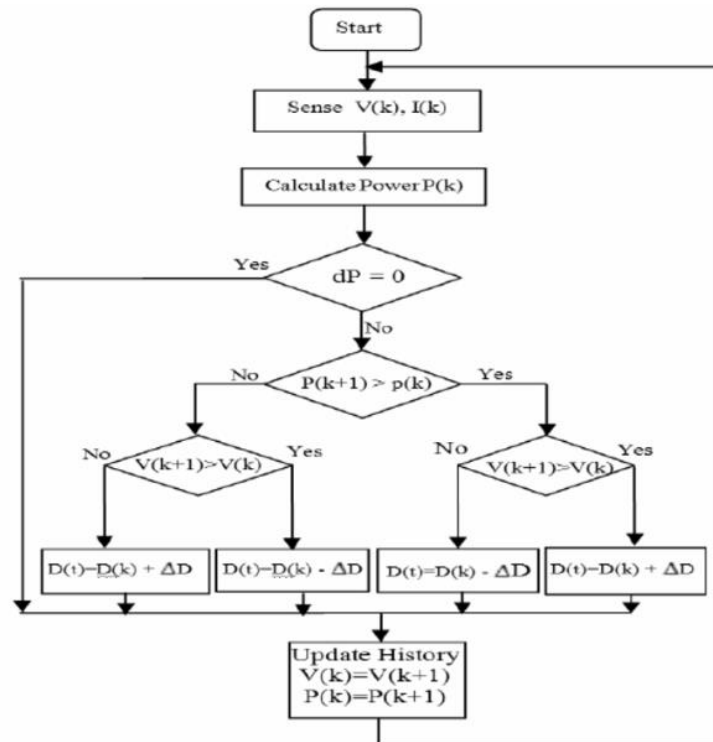


Figure 6: Flowchart for the P&O Method

A flow chart of the P&O method can be found in figure 6.

V. RESULT AND DISCUSSIONS

The P&O-MPPT Managed 10 s SEH System is depicted in figure 7, where the x-axis denotes the passage of time and the y-axis denotes the voltage of the battery. INC-MPPT Managed 10s SEH systems are depicted in figure 8, where the x axis represents time and the y axis represents battery voltage.

The three parameters of the regulated P&O-MPPT and INC-MPPT Battery charger solar energy harvesting means state of charge (SOC), battery current, and voltage are derived in Figures 7 and 8 above for a simulation time of 10s. The P&O-MPPT SOC went down to 8%, while the INC-MPPT SOC went down to 19%. The SOC's have a distinct perspective on the INC-MPPT compared to the P&O-MPPT.

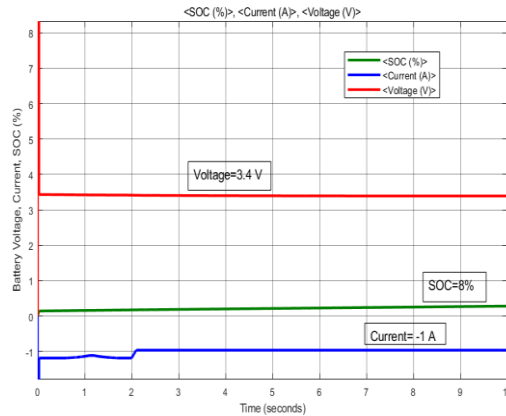


Figure 7: P&O-MPPT Managed 10 s SEH System

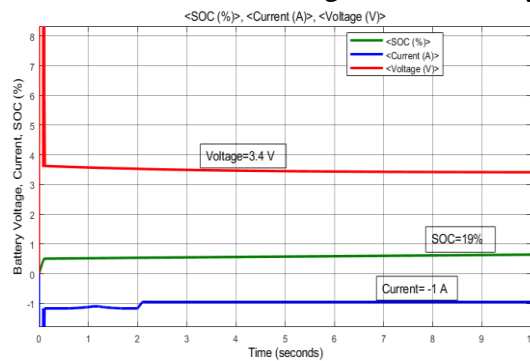


Figure 8: INC-MPPT Managed 10 s SEH systems

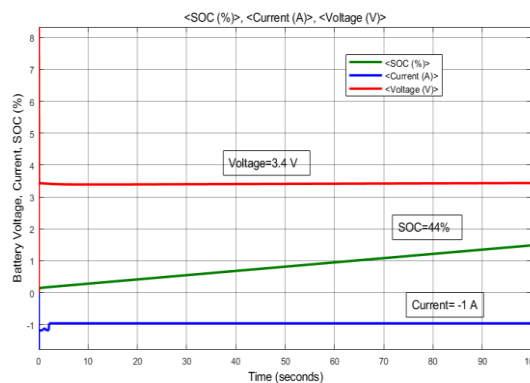


Figure 9: P&O-MPPT managed 100 s SEH system

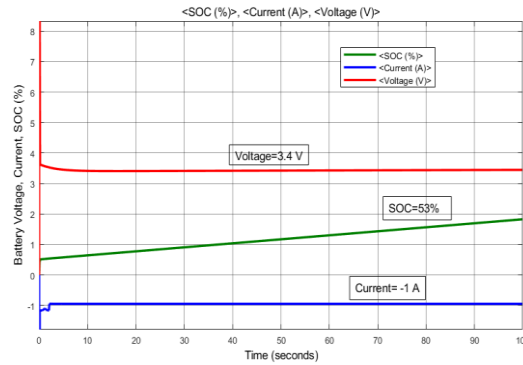


Figure 10: INC-MPPT managed 100 s SEH system

On the x axis of figure 9, the time of a P&O-MPPT managed 100 s SEH system is displayed, and on the y axis, the battery voltage current is displayed. Figure 10 presents an illustration of an INC-MPPT managed 100 s SEH system, with the y axis displaying the battery voltage. Figures 9 and 10 show that all three parameters were determined after running the simulation for a total of one hundred seconds for both P&O-MPPT and INC-MPPT. Both indicate an increase in the level of charge of the battery. The P&O-MPPT SOC achieves a maximum of 44%, whereas the INC-MPPT SOC reaches a maximum of 53%. Once more, the results of different simulation times reveal that INC-MPPT produces a better increment than P&O-MPPT.

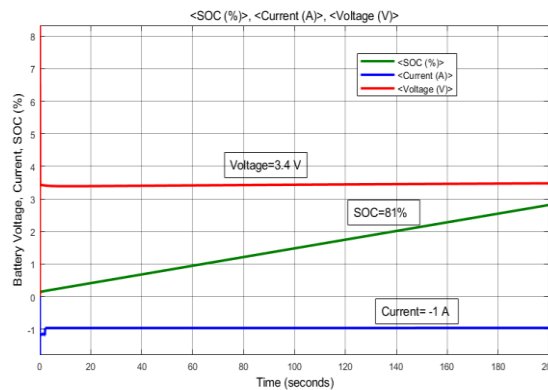


Figure 11: P&O-MPPT Controlled 200 s SEH system

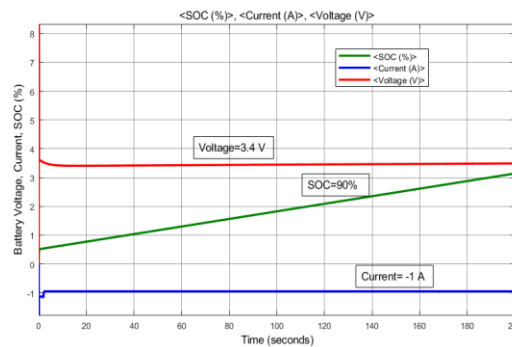


Figure 12: INC-MPPT Controlled 200 s SEH system

Figure 11 depicts, along its x-axis, the amount of time that P&O-MPPT managed 200s SEH systems were in operation, while its y-axis displays battery voltage current. The figure 12

represents an INC-MPPT managed 200s SEH system, while the y axis displays the voltage of the battery.

Again, all three parameters are simulated for the P&O-MPPT and the INC-MPPT in figures 11 and 12, all of which have a simulation time of 200s. Because the passage of time causes the SOC to rise, this occurs automatically. Because of the extended duration of the simulation, the SOC of the P&O-MPPT reaches 80%, whereas the SOC of the INC-MPPT reaches 89%. When compared to P&O-MPPT, the rate of SOC increment that is produced by INC-MPPT is significantly superior.

VI. CONCLUSION

Throughout the course of this research, modeling, simulation, and optimization are carried out for SEH-WSN nodes. Using MATLAB, we were able to simulate both the P&O-MPPT and the INC-MPPT control methods for the solar energy harvester system. This allowed for an in-depth study as well as a comparison of the two. INC-MPPT and P&O-MPPT are simulated at a variety of simulation times, and in each and every case, the results that INC-MPPT produces are superior to those that P&O-MPPT generates. Additionally, the overall efficiency of the P&O-MPPT technique is 87.65%, while the efficiency of the INC-MPPT technique is 90.17%, which is a higher percentage than the efficiency of the P&O-MPPT SEH Controlled approach. Thus, INC-MPPT is highly promising approach. The effectiveness of the work that will be done in the future will be improved by utilizing the other parameters as well. In order to achieve greater efficacy, the other algorithm will be implemented as well.

References

- [1] Cui, R., Qu, Z., & Yin, S. (2013, November). Energy-efficient routing protocol for energy harvesting wireless sensor network. In 2013 15th IEEE International Conference on Communication Technology (pp. 500-504). IEEE.
- [2] Ibrahim, R., Chung, T. D., Hassan, S. M., Bingi, K., & bintiSalahuddin, S. K. (2017). Solar energy harvester for industrial wireless sensor nodes. *Procedia Computer Science*, 105, 111-118.
- [3] Sharma H, Haque A, Jaffery ZA.(2018) An Efficient Solar Energy Harvesting System for Wireless Sensor Nodes. In2018 2nd IEEE International Conference on Power Electronics, Intelligent Control and Energy Systems (ICPEICES) 2018 Oct 22 (pp. 461-464). IEEE.
- [4] Mohamed, S. A., & Abd El Sattar, M. (2019). A comparative study of P&O and INC maximum power point tracking techniques for grid-connected PV systems. *SN Applied Sciences*, 1(2), 174.
- [5] Ahmad, T., Sobhan, S., & Nayan, M. F. (2016). Comparative analysis between single diode and double diode model of PV cell: concentrate different parameters effect on its efficiency. *Journal of Power and Energy Engineering*, 4(3), 31-46.
- [6] Sharma, H., Haque, A. and Jaffery, Z.A., (2018). Solar energy harvesting wireless sensor network nodes: A survey. *Journal of Renewable and Sustainable Energy*, 10(2), p.023704.
- [7] Rasheduzzaman, M., Pillai, P. B., Mendoza, A. N. C., & De Souza, M. M. (2016, July). A study of the performance of solar cells for indoor autonomous wireless sensors. In 2016

- 10th International Symposium on Communication Systems, Networks and Digital Signal Processing (CSNDSP) (pp. 1-6). IEEE.
- [8] Choudhary, D., & Saxena, A. R. (2014). Incremental Conductance MPPT algorithm for PV system implemented using DC-DC buck and boost converter. *Int. Journal of Engineering Research and Applications*, 4(8), 123-132.
- [9] Veerachary, M., & Saxena, A. R. (2011). Design of robust digital stabilizing controller for fourth-order boost DC-DC converter: A quantitative feedback theory approach. *IEEE Transactions on Industrial Electronics*, 59(2), 952-963.
- [10] Baci, A. B., Salmi, M., Menni, Y., Ghafourian, S., Sadeghzadeh, M., & Ghalandari, M. (2020). A New Configuration of Vertically Connecting Solar Cells: Solar Tree. *International Journal of Photoenergy*, 2020.
- [11] Eseosa, O., & Kingsley, I. (2020). Comparative Study of MPPT Techniques for Photovoltaic Systems. *Saudi Journal of Engineering and Technology*, 12-14.
- [12] Liu, L., Oza, S., Hogan, D., Perin, J., Rudan, I., Lawn, J. E., ... & Black, R. E. (2015). Global, regional, and national causes of child mortality in 2000–13, with projections to inform post-2015 priorities: an updated systematic analysis. *The Lancet*, 385(9966), 430-440.
- [13] Kumar, R., Choudhary, A., Koundal, G., & Yadav, A. S. A. (2017). Modelling/simulation of MPPT techniques for photovoltaic systems using Matlab. *International Journal*, 7(4).
- [14] Kinjal, P., Shah, K. B., & Patel, G. R. (2015, January). Notice of Removal: Comparative analysis of P&O and INC MPPT algorithm for PV system. In 2015 International Conference on Electrical, Electronics, Signals, Communication and Optimization (EESCO) (pp. 1-6). IEEE.
- [15] Kumar, M. Kapoor, S. R. Nagar, R., & Verma, A. (2015). Comparison between IC and Fuzzy Logic MPPT Algorithm Based Solar PV System using Boost Converter. *International Journal of Advanced Research in Electrical, Electronics and Instrumentation Engineering*, 4(6), 4927-4939.
- [16] Mathew, A., & Selvakumar, A. I. (2006). New MPPT for PV arrays using fuzzy controller in close cooperation with fuzzy cognitive network. *IEEE Trans. Energy Conv*, 21(3), 793-803.
- [17] Green, M. A., Hishikawa, Y., Dunlop, E. D., Levi, D. H., Hohl-Ebinger, J., & Ho-Baillie, A. W. (2018). Solar cell efficiency tables (version 51). *Progress in photovoltaics: research and applications*, 26(1), 3-12.
- [18] Mathews, I., King, P. J., Stafford, F., & Frizzell, R. (2015). Performance of III-V solar cells as indoor light energy harvesters. *IEEE Journal of Photovoltaics*, 6(1), 230-235.
- [19] Sanchez, A., Blanc, S., Climent, S., Yuste, P., & Ors, R. (2013). SIVEH: Numerical computing simulation of wireless energy-harvesting sensor nodes. *Sensors*, 13(9), 11750-11771.
- [20] Erickson, R. W., & Maksimovic, D. (2007). *Fundamentals of power electronics*. Springer Science & Business Media vol. 1, 2nd pg. 3-14.
- [21] Pathak, G., Saxena, A. R., & Bansal, P. (2014). Review of dimming techniques for solid-state LED lights. *International Journal of Advanced Engineering Research and Technology (IJAERT)*, 2(4), 108-114.

- [22] H. Al-Bahadili, H. Al-Saadi, R. Al-Sayed, M.A.-S. Hasan, (2013), "Simulation of maximum power point tracking for photovoltaic systems", Applications of Information Technology to Renewable Energy Processes and Systems (IT-DREPS), 1st International Conference & Exhibition, 2013,79-84.
- [23] Hauke, B. (2009). Basic calculation of a boost converter's power stage. Texas Instruments, Application Report November, 1-9.
- [24] Texas Instruments Application Report on "Calculating Efficiency of PMP-DC-DC Controllers". Available online: www.ti.com (accessed on 28 June 2018).
- [25] Haque, A. (2014). Maximum power point tracking (MPPT) scheme for solar photovoltaic system. Energy Technology & Policy, 1(1), 115-122.